JOURNAL OF SPACECRAFT AND ROCKETS
Vol. 38, No. 3, May–June 2001

Design Considerations for Cryogenic Pumping Arrays in Spacecraft–Thruster Interaction Facilities

Andrew D. Ketsdever*
U.S. Air Force Research Laboratory, Edwards Air Force Base, California 93524

In general, the simulation of the space environment in ground-based facilities poses many challenges, and the study of propulsion-system-induced effects on spacecraft poses additional challenges to a facility's design due to the complex nature of thruster flows. Low facility background pressures at high mass flow rates are required to obtain meaningful interaction data. Although there is some history to draw from for the design of space simulation chambers, there are very few design philosophies for thruster–spacecraft interaction facilities. This study explores some of the more interesting design philosophies for spacecraft–thruster interaction facilities and offers general guidelines for future designs.

Nomenclature

A = area, m^2
$c(\gamma)$ = constant based on γ
D = characteristic diameter, m
F_r = fraction of molecules returning to thruster area after interacting with pumping surfaces
f_p = fraction of facility inner surface occupied by pumping
h = radial fin array height, m
I = ion current, A
I_n = column depth, m^{-2}
I_{sp} = specific impulse, s
k = Boltzmann's constant, 1.38×10^{-23} J/K
L_c = largest internal facility dimension, m
$\dot{M}$ = mass flow, kg/s
n = number density, m^{-3}
p = pressure, Pa
r_p = radius of penetration, m
T = temperature, K
t = radial fin array panel thickness, m
$\dot{V}$ = facility volumetric pumping speed, m^3/s
v = velocity, m/s
v' = mean thermal velocity, m/s
w = radial fin array panel spacing, m
x = axial distance downstream of thruster exit plane, m
γ = ratio of specific heats
η = sticking coefficient
κ = constant (on the order of 10^7 in SI units)
λ = mean free path, m
σ = collision cross section, m^2
$\Im$ = thrust, N

Subscripts

a = cryogenic pumping array
b = background gas
cx = charge exchange
if = fast ions
io = ions at thruster exit plane
is = slow ions
p = plume gas
rf = radial fin array
s = surface
sw = smooth wall or cylindrical array
t = thruster
ts = test sphere
wf = wedge fin array
0 = thruster stagnation or initial

Presented as Paper 2000-0463, at the AIAA 38th Aerospace Sciences Meeting, Reno, NV, 10–13 January 2000; received 26 April 2000; revision received 2 January 2001; accepted for publication 5 January 2001.

*Senior Research Engineer, Advanced Concept and Propulsion Sciences Division, Propulsion Directorate, 10 E. Saturn Boulevard; andrew.ketsdever@edwards.af.mil. Member AIAA.

Introduction

THE interactions between onboard spacecraft propulsion systems and spacecraft surfaces has received considerable attention in recent years from Department of Defense, NASA, and commercial investigators.[1,2] The growing popularity of electric ion propulsion systems promises renewed interest in this area of research. The impact of potential interactions on spacecraft is becoming more critical as mission life and payload sensitivity requirements are continually increased. The adsorption of propellant gases on spacecraft surfaces (often referred to as contamination) can change solar absorptivity of thermal control surfaces, alter reflectivity of optical surfaces, alter transmission through solar cell coverglass, and induce environments that can alter scientific results. Ion electric thrusters add further complications due to material sputtering from high-energy ion (propellant) impact and the possible alteration of spacecraft potentials.[3]

Although the space shuttle has made space-based investigations more feasible by providing a reliable space platform and the capability of returning payloads to Earth for careful examination, the cost of space-based experiments is still prohibitively high. Space-based experiments can also be extremely limited in scope due to a lack of available instrumentation, geometrical variation, accurate detail of the time-dependent space environment, and on-orbit time. It is clear that ground-based examination of thruster–spacecraft interactions is necessary to compliment the sometimes limited data returned from space experiments.

Some of the immediate advantages to having ground-based facilities include the reduced cost of obtaining data, the ability to change experimental configurations, the ability to perform tests with a large number of material samples, the ability to perform accelerated testing for material certification, and the availability of a greater array of diagnostic tools. The major disadvantage of ground-based facilities is obvious. To date, the daunting challenge of ground-based facilities has been the faithful reproduction of the space environment. The limitation of ground-based facilities in accurately predicting the effects of thruster operation on spacecraft systems has always been driven by the facility's background pressure.[4,5] There are at least three components of the background pressure with which a facility must contend. Although some fraction of the background gas is composed of the residual laboratory atmosphere, the largest complication can arise from that the overwhelming majority of the background gas is thruster derived. These thruster-borne components of the background gas are largely responsible for experimental measurement errors. Besides the thruster effluents and residual atmosphere, ion electric thrusters can also produce a third background population

of sputtered products due to high-energy ion impact with thruster and chamber surfaces. The effects of the residual atmosphere can be minimized by operating the facility at very low ultimate pressure. Although achieving low ultimate pressure in a large vacuum facility can be difficult, minimizing the effects of thruster-borne effluents is much more complicated.

A distinction should be drawn between thruster test facilities (performance and lifetime) and spacecraft–thruster interaction facilities. For thruster performance and lifetime measurements, maintenance of adequate background pressures and facility operating costs are the driving factors that determine facility design. However, spacecraft–thruster interaction studies require more efficient pumping schemes. Because spacecraft propulsion systems are typically not designed to impinge directly on spacecraft surfaces, interaction studies are characterized by a need to investigate the far-field and high-angle or backflow plume regions. Typically, plume densities are rather low in these regions, which increases facility pumping requirements significantly, and in some cases, the background pressures in interaction facilities are required to be orders of magnitude lower than in thruster performance and lifetime facilities.[1] The critical facility operating characteristics for interaction studies are the suppression of thruster effluents scattering from chamber surfaces and the maintenance of low facility background pressures. Therefore, improvements to the accuracy of ground-based interaction data come at the cost of more efficient chamber pumping. This paper explores several possibilities for improved facility pumping for both chemical and electric thrusters that may allow more accurate spacecraft–thruster interaction studies.

Historical Perspective: Ground-Based Facilities

Although not intended to be an exhaustive survey of ground-based thruster facilities, this section details some of the more prevalent facilities that utilize specially designed cryogenic pumping arrays. A distinction should be made between facilities designed for performance and lifetime testing and spacecraft–thruster interaction facilities. In general, spacecraft–thruster interaction facilities require specialized pumping because backscattered molecules from chamber walls must be minimized. As discussed in subsequent sections, pumping schemes that cover the entire inner surface of a facility are required to effectively minimize thruster effluent backscattering. To this end, the discussion in this section will address the following facilities: the Space Molecular Sink (MOLSINK), Jet Propulsion Laboratory (JPL) in Pasadena, California; STG, DLR, German Aerospace Research Center in Gottingen, Germany; and Chamber-IV of the Collaborative High Altitude Flow Facility (CHAFF-IV), University of Southern California (USC), Los Angeles, California.

MOLSINK Facility

The MOLSINK facility at JPL was constructed during the mid- to late-1960s and has since been dismantled; however, its innovative design and the unique data collected in this facility have endured. The MOLSINK's wedged cryogenic fin array, shown schematically in Fig. 1, was enclosed within a 3-m-diam stainless steel chamber. The wedged fin array was exposed to an operating thruster and was capable of cryopumping thruster effluents.[6] The cryopumped array was cooled to 21 K by a 1000-W gaseous helium refrigerator. The unique characteristic of the cryopumping system was the 2.4-m-diam wedge fin molecular trap (moltrap) array, which provided 186 m^2 of pumping area. The angles of the fins were such that their projections were tangent to a 25.4-cm sphere at the center of the moltrap. This design was shown to have an order of magnitude capture improvement over a smooth-wall capture when the thruster operated within the 25.4-cm sphere in the center of the array.

Investigators calculated that, if a spherical source were contained completely within the 25.4-cm-diam imaginary sphere at the center of the array, only 35 of every 100,000 molecules emitted from the source would return to the source.[6] This analysis assumed a cryopumping capture coefficient of 0.70 on the array. Molecular hydrogen and helium was pumped by means of a titanium sublimation pump. The electron-beam sublimator was mounted on the inner door of the chamber and allowed approximately 7×10^6 l/s of hydrogen to be pumped.[7] Several thruster interaction experiments were carried out in the MOLSINK facility. These tests examined the backscattering of nozzle exhaust plumes[7,8] and simulated chemical thrusters.[9]

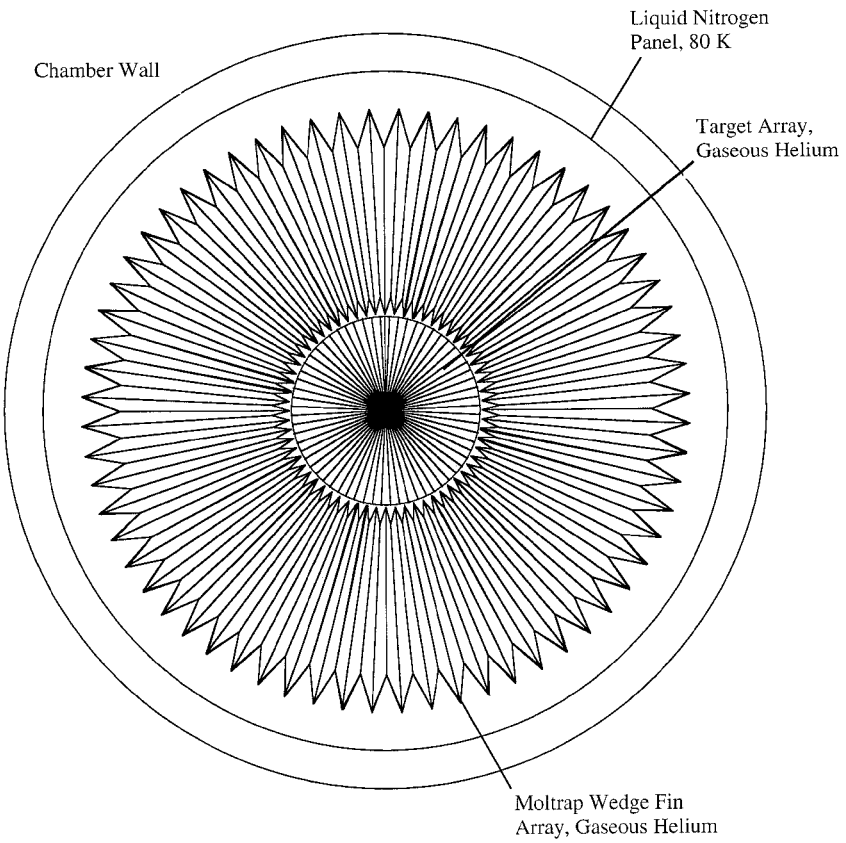

Fig. 1 Top view of the wedge fin cryogenic pumping array of the JPL Molsink facility.

Table 1 Sticking coefficients of some common gases as a function of gas and surface temperature (adapted from Ref. 11)

Cryosurface temperature, K	N_2		CO		O_2		Ar		CO_2	
	77 K	300 K	77 K	300 K	77 K	300 K	77 K	300 K	77 K	300 K
10	1.0	0.65	1.0	0.90	——	——	1.0	0.68	1.0	0.75
12.5	0.99	0.63	1.0	0.85	——	——	1.0	0.68	0.98	0.70
15	0.96	0.62	1.0	0.85	——	——	0.9	0.67	0.96	0.67
17.5	0.90	0.61	1.0	0.85	1.0	0.86	0.81	0.66	0.92	0.65
20	0.84	0.60	1.0	0.85	——	——	—— 0.80	0.66	0.90	0.63
22.5	0.80	0.60	1.0	0.85	——	——	0.79	0.66	0.87	0.63
25	0.79	0.60	1.0	0.85	——	——	0.79	0.66	0.85	0.63
77	——	——	——	——	——	——	——	——	0.85	0.63

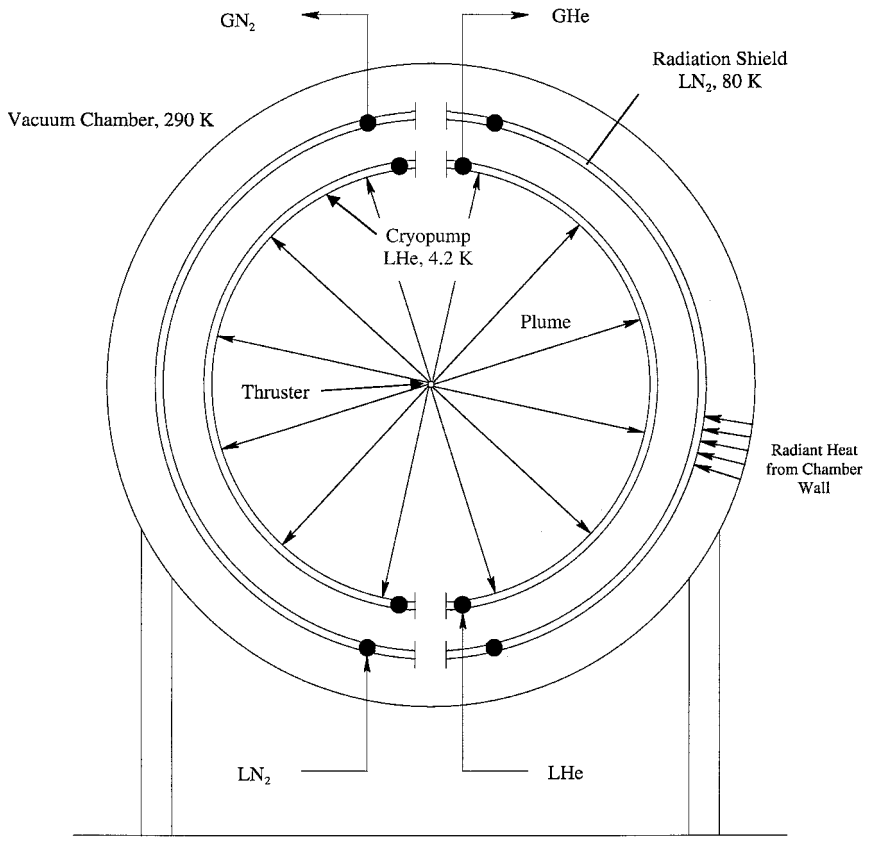

Fig. 2 Front view of the cylindrical cryogenic pumping array of DLR plume test facility STG.

STG Facility

The STG facility at DLR became operational in 1997. The chamber is 3.3 m in diameter and 7.6 m long. It is cryopumped using a smooth walled, cylindrical panel system shown in Fig. 2, which provides 30 m^2 of pumping area (5.25 m long $\times$ 1.6 m diam).[10] The cryopumping is accomplished by supplying the inner cryopanels with liquid helium. As shown in Table 1,[11] the effective sticking coefficient of a propellant molecule on a cryopumping surface is a function of both the propellant molecule's temperature and the temperature of the pumping surface. Therefore, liquid helium cryogen at approximately 4 K will pump more efficiently (larger sticking coefficient) than other conventional means of cryogenic pumping at a given propellant temperature. Also, liquid helium allows for the pumping of molecular hydrogen, which cannot be condensed on surfaces using gaseous helium cryostats. The outer cylindrical panel closest to the chamber walls are supplied with liquid nitrogen at 77–80 K. This outer panel acts to minimize the radiative heat transfer from the room temperature outer walls of the chamber to the inner cryopumping panel supplied with liquid helium at 4.2 K. Initial experiments using high Reynolds number nozzles operating on N_2 and H_2 have been reported.[12]

CHAFF-IV

CHAFF-IV is part of CHAFF at USC. Although not yet completed at the time of this paper, the facility is partially operational and has undergone initial performance testing.[13] CHAFF-IV consists of a cryogenic radial fin array system encased in a 3-m-diam by 6-m-long vacuum chamber. The fabricated radial fin cryopanel arrays are shown in Fig. 3. The finned array is similar to that use by the MOLSINK facility with one exception. Instead of a wedged fin arrangement, CHAFF-IV utilizes an opened radial fin system that allows for the operation of ion electric thrusters within the chamber. The MOLSINK arrangement would not allow for ion electric thruster operation due to energetic ion sputtering of the cryopanel material subjected to direct impingement of thruster effluents.

The cryogenic fin arrangement, which covers the entire chamber inner surfaces, allows CHAFF-IV approximately 590 m^2 of pumping area. The cryopanels are cooled to 15–20 K by a 900-W gaseous helium refrigerator. The radial fin array also allows heat dissipated by an operating thruster to impinge on the liquid nitrogen outer shield instead of on the cryorefrigerated panel system. The open fin geometry effectively increases the maximum power level of an electric thruster to approximately 3.5 kW in CHAFF-IV, while still

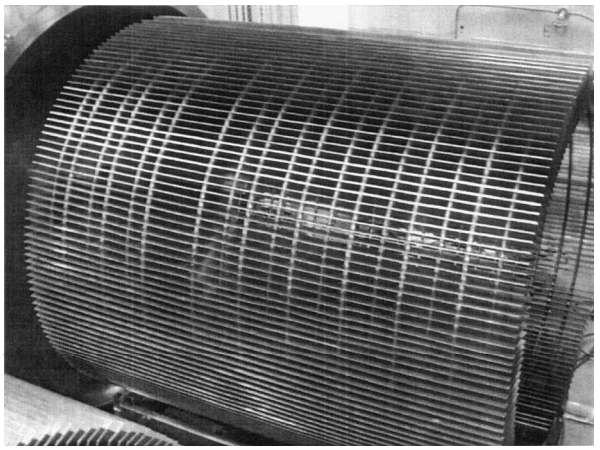

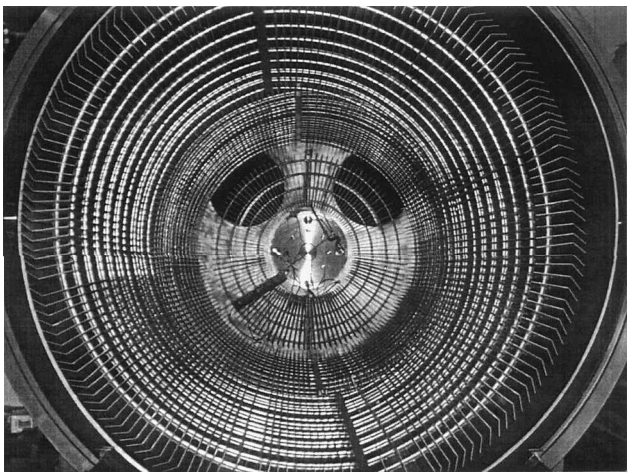

Fig. 3 Fabricated radial fin cryopanel array installed in the USC CHAFF-IV (photographs courtesy of USC).

maintaining adequate panel temperature to ensure xenon pumping.[14] Initial experiments have been performed in CHAFF-IV to assess the facility's ultimate pumping speed. Initial experiments indicate that the pumping speed should exceed 9×10^6 l/s for cold gas flows.[13,15] Actual thruster pumping rates will vary depending on power dissipation, degree of propellant ionization, and sputtering rates.

Requirements for Ground-Based Interaction Studies

To assess the effects of thruster effluents expanding into a finite pressure (background gas), a simple physical model will be incorporated.[16] Although this discussion was originally framed in terms of conventional nozzle expansions, it is generic enough to apply to ion electric thrusters. The thruster exhaust has two primary characteristic dimensions: the mean free path λ_p of the exhaust gases in the background gas and the distance from the thruster, r_p, in which the plume is free from background gas penetration (also known as the radius of penetration).

On the thruster centerline, the radius of penetration can be given by[17]

$$r_p = (v_r/v_b')\pi(\sigma)^2 n_0 c(\gamma) D_t^2 \tag{1}$$

where $v_r = v_p + v_b'$ and σ is the combined collision cross section between the plume and background species. Equation (1) can be simplified into convenient propulsion terms by

$$r_p = \kappa\left(\Im/v_p^2\right) \propto 1/I_{\text{sp}}^2 \tag{2}$$

For ion electric thrusters operating at high specific impulse ($I_{\text{sp}} \sim 1600$ s), the background gas in a facility is able to penetrate freely up to the exit plane and even into the discharge region of the thruster.

The plume mean free path in a background gas is given by

$$\lambda_p = 1/\sqrt{2}\sigma n_b \tag{3}$$

For ion electric thrusters, the shortest mean free path is due to charge exchange because the charge exchange cross section is larger than that for momentum exchange. From this arrangement, a plume Knudsen number can be defined by

$$Kn_p = \lambda_p/r_p \tag{4}$$

If $Kn_p \gg 1$, the interactions between the plume species and the background gas can be considered as two separable scattering events. The first event is the effective stopping of the exhaust gas relative to the background gas in a distance λ_p, and the second is the diffusive penetration of the background gases into the plume up to a distance of r_p. For thruster interaction facilities, it is important to keep Knudsen number Kn_p close to space conditions in the areas of interest in the plume most notably in the far plume and high-angle (from thruster centerline) regions.

Special Issues Associated with Nozzle Expansions

Nozzle expansions are typically operated at relatively high Reynolds numbers in an attempt to maintain propulsive efficiency, which can translate to very high propellant mass flow rates expanding into a ground-based facility. Nozzle expansion thrusters are typically used on spacecraft for high thrust orbital maneuvering. Note that by Eq. (2) the radius of penetration can be quite large for a nozzle expansion. In other words, penetration of the background gas into the plume occurs only after several nozzle diameters downstream of the exit plane. The resulting plume flow for a nozzle expansion in space and ground-based facilities[18] is shown in Fig. 4. As a consequence, the background pressure and composition for studying nozzle expansions in the core of the flow (inside dashed line in Fig. 4a) are not particularly critical.

However, for interaction studies between nozzle expansions and spacecraft surfaces, the background pressure is absolutely critical for two reasons. First, the fluid mechanical nature of the impinging flow on a surface is fundamentally different for continuum and free molecule conditions near a wall, as shown in Fig. 5. In space, the entire range of continuum flow through transition and subsequent free molecule flow is experienced. To satisfy the free molecule flow condition low background pressures are required.[19] The second reason for desired low background pressure facility operation with nozzle expansions is plume backflow, shown in Fig. 6. (Ref. 18) Plume backflow is primarily determined by a thin subsonic boundary layer near the nozzle lip, which can turn sharply at the lip while undergoing expansion. Once in the backflow region, the flow very quickly becomes free molecular.[18] Again, to reproduce faithfully nozzle backflow characteristics in ground-based facilities, low operating background pressure and efficient pumping of exhaust species is required. As shown in Fig. 4 , there is a need for pumping schemes that cover the entire inner surface of a facility to accomplish these tasks.

Because of the high flow rates exhausting from nozzle expansion thrusters, effective cryopumping can be difficult to maintain. Depending on the propellant mass flow, the heat flux from the propellant gases to the cryogenic arrays can be quite high and can easily overwhelm the capacity of a typical cryostat. There are several other special issues associated with the ground-based testing of nozzle expansion thrusters including the pumping of relatively large amounts of hydrogen formed during the combustion process of chemical thrusters. Hydrogen is difficult to pump cryogenically without the aid of cryosorption material (zeolite) or effective sublimation pumping. The pumping of incondensable gases is described in detail in a following section. Also, plume contamination on spacecraft surfaces due to self-scattering (propellant molecules colliding in the plume) can be important for sensitive subsystems.[9] Adequate background pressures are required for these studies, which do not significantly increase the propellant's collision probability in the plume at reasonable distances downstream of the thruster exit plane.

Special Issues Associated with Ion Electric Propulsion Systems

As can be seen from Eq. (2), the background gas in a facility is able to penetrate freely up to exit plane of an ion electric thruster. Investigations of ion electric thruster operations in ground-based facilities are likely to be extremely sensitive to facility-induced background

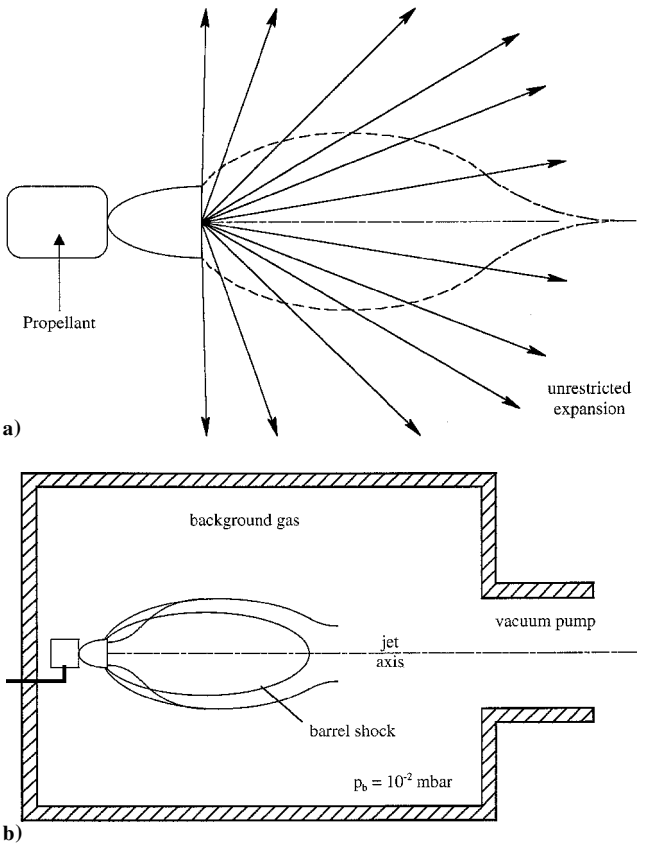

Fig. 4 Plume expansion in a) space, b) vacuum chamber with conventional pumping, and c) vacuum chamber with cryogenic pumping (adapted from Ref. 18).

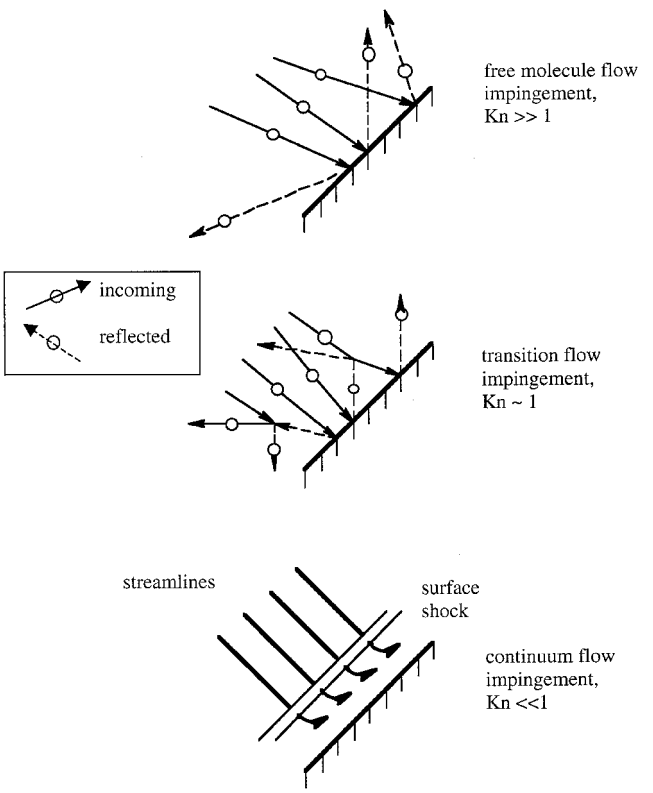

Fig. 5 Plume impingement on surfaces (adapted from Ref. 18).

populations. In fact, such effects may be very subtle because the propellant gas (in most cases xenon) is the same as the generated background gas.

Entrained Gas Flow

With a xenon background gas capable of penetrating to the thruster exit plane, background gas can be entrained into the discharge region of the thruster and reused as propellant. Entrained propellant flow can result in performance enhancement because the effective thrust is increased without accounting for the increase in propellant mass flow.[20] Because the entrainment flux of background gas to the thruster is proportional to the background gas number density, adequate pumping is required to reduce its effects on performance measurements. Randolph et al.[20] suggest that the entrained mass flow rate should be less than 3% of the injected propellant flow rate to obtain accurate measurements. From a simple analysis, it is found that the chamber pressure should be below 5×10^{-5} torr to ensure this condition for a typical Hall effect thruster, that is, a stationary plasma thruster SPT-100. The entrainment of background gases has also been observed to induce discharge oscillations that can severely degrade thruster performance.[21] These oscillations can occur at background pressures of approximately 3×10^{-5} torr. The obvious recommendation is to maintain facility background pressures below this value.

Charge Exchange

In the single charge exchange process, a fast moving ion from the thruster discharge interacts with a relatively slow moving neutral atom or molecule exchanging their charge and a small amount of kinetic energy. The result is a fast moving neutral atom and a slow ion from reaction 1:

$$X^+_{\text{fast}} + Y_{\text{slow}} \rightarrow X_{\text{fast}} + Y^+_{\text{slow}} + \Delta E$$

where ΔE is the energy defect of the process or the difference of the two atoms ionization potential.[22] In the case of a fast xenon ion expelled into a slow xenon background gas, the energy defect is zero. This condition is known as a resonant charge exchange, and the cross section for resonant charge exchange collisions σ_{cx} can be quite large. Recent results by Pullins et al.[23] give a charge exchange cross section for xenon ions at 300-eV energies with thermal xenon atoms of 55 Å^2.

Because the background number densities in ground-based facilities is much larger than experienced on-orbit, dramatic increases in charge exchange collisions are expected. Increased charge exchange collisions in ground-based facilities can cause two fundamental problems in trying to assess plume interaction effects. First, the primary ions in the main thruster beam will be depleted by

$$I_{cx} = I_0 \exp(-n_b \sigma_{cx} x) \tag{5}$$

where I_{cx} is the primary ion current collected at an axial position x downstream of the exit plane. For a background pressure of 5×10^{-5} torr, the primary ion beam 1 m downstream of the thruster exit plane is expected to be reduced by over 55% of the initial beam current.

The second major effect of increased charge exchange collisions in ground-based facilities is the creation of a large number of slow moving ions. It is generally known that slow moving charge exchange ions are capable of being transported back toward spacecraft.[24] The relatively low-energy charge exchange ions can

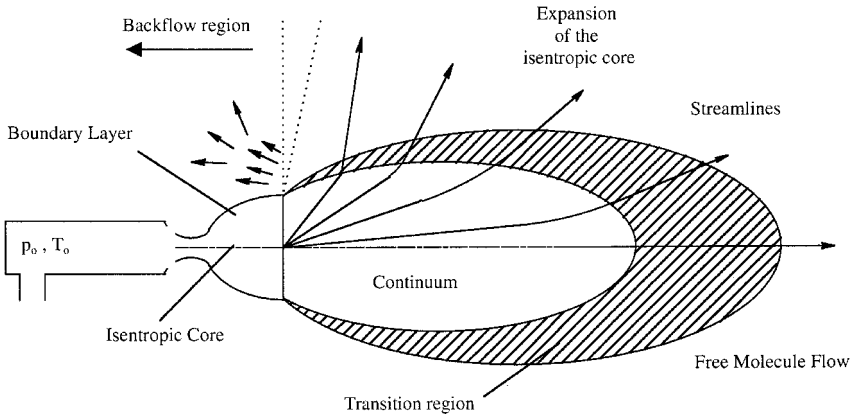

Fig. 6 Flow types in a plume expanding into vacuum (adapted from Ref. 18).

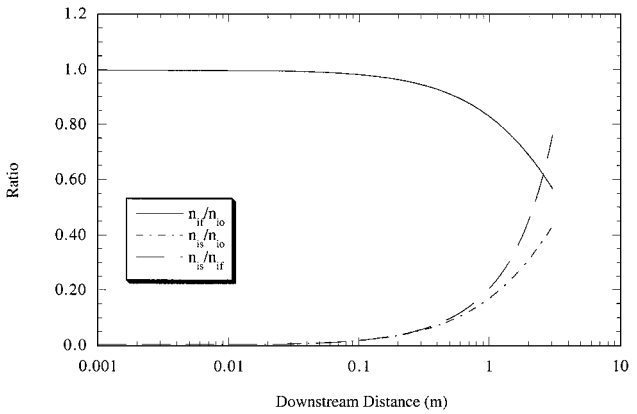

Fig. 7 Charge exchange populations as a function of distance from an ion thruster exit plane for $p_b = 1 \times 10^{-5}$ torr.

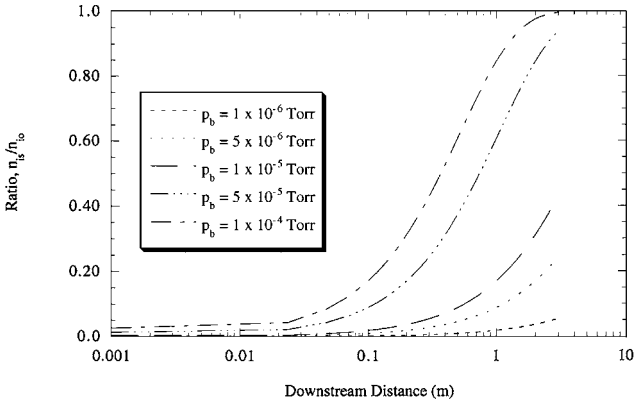

Fig. 8 Fraction of charge exchange ions to primary ions as a function of distance from an ion thruster exit plane and background pressure.

be influenced by local electric fields in the plume and near spacecraft. The creation of charge exchange ions for the case of fast ions impinging on a slow background gas target is given by[17]

$$d(n_{is}) = (n_{if}\sigma_{cx} - n_{is}\sigma_r)\, dI_n \tag{6}$$

where σ_r is the recombination cross section.

For resonant charge exchange collisions at relatively low pressures, $\sigma_{cx} \gg \sigma_r$ due to the lack of three-body collisions in the plume. It has also been found that the collision (or momentum transfer) cross section for xenon ions colliding with neutral xenon is an order of magnitude smaller than σ_{cx} (Ref. 25). Based on these assumptions, the solutions to Eq. (6) are

$$n_{is}/n_{io} = (1 - e^{-\sigma_{cx} I_n}) \tag{7}$$

$$n_{if}/n_{io} = e^{-\sigma_{cx} I_n} \tag{8}$$

$$n_{is}/n_{if} = (1 - e^{-\sigma_{cx} I_n})/e^{-\sigma_{cx} I_n} \tag{9}$$

where n_{io} is the initial number density of ions at the thruster exit plane where $I_n = 0$.

Figure 7 shows the effects of charge exchange on the primary ion beam of a ion electric thruster for a background pressure of 1×10^{-5} torr. Figure 8 shows the ratio of Eq. (7) for various background pressures. As shown in Fig. 8, the charge exchange population of slow ions increases dramatically for increased background density quite close to the thruster exit plane. For this reason, interaction studies that investigate the effects of charge exchange ions in the backflow regions must be carried out at very low background pressures.

Facility Design

In a typical ground-based facility with a fraction f_p of its inner surface occupied by pump inlets, the thruster effluents are generally

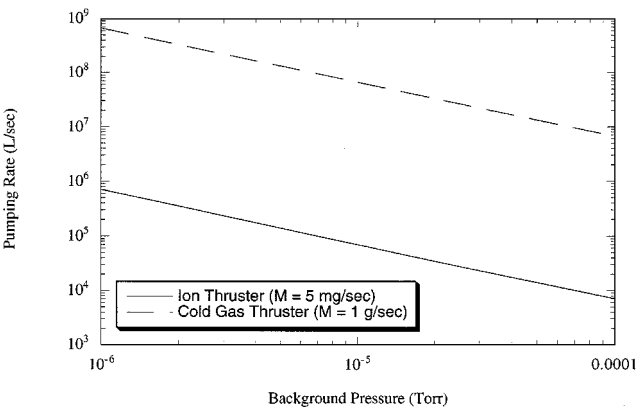

Fig. 9 Facility pumping speed to maintain a given background pressure for a typical Hall (ion) thruster flow (Xe) and cold gas thruster (N_2).

stopped and randomized by the facility's surfaces. The random motion of the scattered propellant molecules drives them into the pump inlets or to a pumping surface. The background number density of propellant gas in a typical facility can be approximated by

$$n_b = \frac{4\dot{M}_p (T_p/T_b)^{\frac{1}{2}}}{m_p v_b' f_p A_s} \tag{10}$$

As we have seen, a driving factor for ground-based thruster interaction studies is maintaining low background pressure during thruster operation. The facility background pressure can be found by

$$p_b = \dot{M}_p k T_b / m_p \dot{V} \tag{11}$$

Figure 9 shows the expected pumping speed to maintain a given background pressure for a typical Hall thruster ($\dot{M} \sim 5$ mg/s of

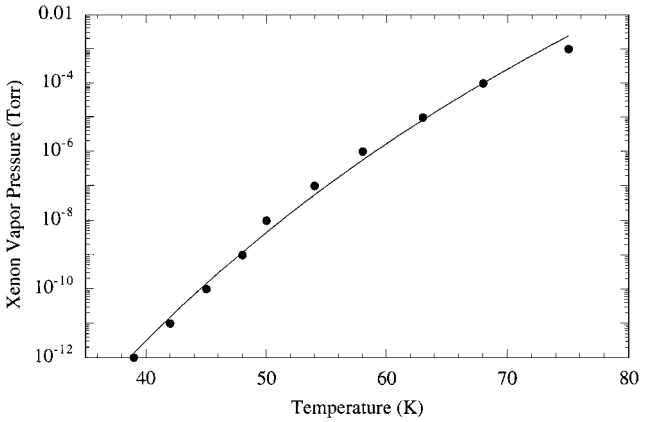

Fig. 10 Vapor pressure–temperature curve for xenon.

xenon) and a cold gas thruster ($\dot{M} \sim 1$ g/s of nitrogen). As indicated in Fig. 10, a pumping rate of approximately 2.5×10^4 l/s is required to maintain a background pressure below 3×10^{-5} torr for the Hall thruster. However for interaction studies where chamber-induced charge exchange collisions must be negligible, an order of magnitude lower background pressure is desired. From Fig. 9, a pumping rate of 2.5×10^5 l/s would required to minimize chamber-induced charge exchange collisions in the far plume or at high angles from the thruster centerline.

For the cold gas system, pumping rates on the order of 10^7 l/s are required to maintain pressures in the 10^{-5} torr range. Pressures on this order are critical to perform high-fidelity backflow measurements. In space, a propellant molecule in the backflow region would most likely encounter a spacecraft surface (up to several meters away) before colliding with another propellant molecule. Free molecular flow (large mean free path) in the plume backflow region must be maintained, which can be effectively accomplished by a background pressure on the order of 10^{-5} torr. Clearly a critical background number density for thruster plume interaction studies is reached when the background mean free path becomes less than or equal to the largest internal dimension of the facility L_c. Therefore, the background number density should be kept at or below

$$n_b \leq 1/\sqrt{2}\sigma L_c \tag{12}$$

For a xenon background gas, the background number density should be $n_b \leq 7 \times 10^{18}\ (L_c)^{-1}$. Depending on the application, it is obvious from the preceding analysis that facility pumping rates between 2.5×10^5 and 10^7 l/s are required for accurate simulation of thruster interactions with spacecraft systems.

Total Chamber Pumping

Total chamber pumping (TCP) is a propellant pumping scheme in which all of the inner surfaces of a facility are utilized as pumping surfaces. TCP can be effective in spacecraft–thruster interaction facilities for two main reasons. First, background gas number densities are minimized by having large available pumping areas ($f_p A_s$) as Eq. (10) indicates. For a given chamber geometry A_s, the pumping rate is maximized by maximizing the fraction of the inner surface area that acts as a pump, that is, $f_p \geq 1$. Therefore, effective pumping is achieved when the entire inner surface of the vacuum facility is a pumping surface. The TCP concept has driven the design of the interaction facilities described earlier.[6,12,14] For chambers that do not utilize TCP, the maximum f_p is on the order of 0.1 due to the limitations of attaching pumps to the external surfaces of a chamber.[26,27] Additionally, TCP offers a similar advantage of increasing pumping speed by replacing the thermal velocity in the denominator of Eq. (10) with the propellant molecule's velocity in the plume. In TCP concepts, it is the plume velocity that brings the propellant molecules to the pumping surfaces as Fig. 4c indicates. Because the plume velocity is much greater than the scattered molecules' thermal speed acquired from the surface (assuming full accommodation), the effective pumping speed of the facility can increase dramatically. The increase in pumping speed is significant only for pumping configurations that utilize TCP because thermalization due to chamber wall collisions dominants in other configurations, that is, $f_p \ll 1$ traditionally.

Second, TCP offers the advantage of minimizing backscattering from chamber surfaces. In the far-field and backflow regions, the plume densities can be orders of magnitude lower than at the thruster exit plane. These regions of great interest for interaction studies are susceptible to background gas penetration as Eqs. (1–4) indicate. Penetration of background gas acts to modify the plume flowfield structure through collisions. To minimize backscattering, it is desirable to have propellant molecules that strike a facility surface effectively pumped on their first interaction with the surface. Because the sticking coefficient for most propellants or products on typical cryogenic surfaces is not equal to one (Table 1), the geometry of the pumping array must aim to reduce the line-of-sight transport of the backscattered molecule to regions of interest. Geometries that encourage multiple surface interactions (on average) before a scattered molecule can find its way back into a volume of interest are obviously advantageous. If the propellant molecule's accommodation to the cryogenic surface is relatively high, the sticking coefficient for interactions subsequent to the initial surface collision will likely be approximately one.

Perhaps the only effective means of implementing TCP is through cryogenic pumping. Cryogenic panels can be fitted into a facility quite easily with supply manifolds for the cryogenic fluid (typically gaseous or liquid helium). The following sections will detail some of the design considerations for cryogenic panels in ground-based interaction facilities.

Cryogenic Pumping Considerations

Note that pumping speeds in cryogenic TCP chambers are limited only by the amount of pumping area available. Conventional pumping systems have a fundamental pumping speed limit that is governed by the conductance of gas through a tube (in this case the tube is the vacuum chamber), as shown in Fig. 4b.[28] There are two important concepts for cryopumping systems. The first is the vapor pressure of a condensed solid on a cryopumping surface as a function of the surface temperature. The vapor pressures for most gases of interest either as atmospheric constituents, propellant species, or thruster products require cryogenic pumping temperatures below 25–30 K for vapor pressures on the order of 10^{-6} torr (Ref. 29). Obviously, lower pumping surface temperatures result in lower possible facility background pressures. Figure 10 shows the vapor pressure of xenon as a function of cryogenic pumping temperature.[30] That xenon vapor pressures below 10^{-6} torr can be achieved for pumping temperatures in excess of 55 K allows for some flexibility when conducting ion electric thruster interaction experiments.

The second important cryopumping concept is that of the sticking or capture coefficient of a gas on the pumping surface. The sticking coefficient is a measure of the probability per collision for a molecule to adsorb on a surface. The sticking coefficient is dependent on the temperature (average kinetic energy) of the gas and the temperature of the cryopumping surface. The sticking coefficients for several gases are given in Table 1.[11] The general trend is toward lower sticking coefficients at higher gas and surface temperatures as expected. As monolayers of adsorbed molecules build on cryogenic surfaces, the sticking coefficient can be adversely affected. Temperature gradients through the adsorbed layers can be significant making the effective surface temperature higher than the actual cryogenic pumping surface.

The major concern for cryopumping systems is heat transfer from propellant gas conduction and radiation from relatively hot chamber and thruster surfaces. The radiation problem can be solved by placing a secondary surface between the room temperature chamber walls and the cryogenic pumping surfaces. The secondary surface is typically cooled with liquid nitrogen so that the radiative energy is from 77 K instead of from 300 K. Other techniques such as highly polished surfaces (to decrease panel absorptivity) and multilayer insulation (mylar sheets, for example) can also help reduce the heat load to a cryogenic panel system. Gas conduction to the cryopanel system can be reduced in a similar manner. Forcing energetic propellant molecules to interact with alternate surfaces (perhaps actively

cooled) before the cryogenic pumping panels can reduce the heat load to the panels significantly. However, an increase background gas population can arise if this is not done properly. Limiting heat transferred to the cryogenic pumping system is critical for maintaining low pumping temperatures because most cryostats (refrigerators) have a finite amount of energy that can be absorbed by the cryogen while maintaining a given temperature.

If possible, contingencies for the introduction of liquid helium should be provided to the cryopanel system to provide supplemental cooling. Because the gaseous helium cryostat system must be a closed loop, this generally needs to be done through an independent feed system. The independent system can also be used to precool the cryopanel array to 77 K with liquid nitrogen, thereby reducing the cooling time required to achieve adequate pumping temperatures. Although the cost of liquid helium is quite high (a factor of 16 times more than liquid nitrogen), the use of liquid helium cryogen can be instrumental in maintaining adequate array pumping temperatures, thus allowing tests of high-power thrusters for short periods of time.

Cryogenic Array Design

Because total pumping surface area is a driving design consideration for interaction facilities, it is instructive to look at concepts for maximizing the pumping area of a cryogenic array. Cryogenic arrays fall into three main categories: smooth wall (cylindrical),[12] radial fin,[14] and wedge fin.[6] These configurations are shown in Fig. 11 and must be visualized in an overall cylindrical configuration, that is, conforming to the inner chamber wall, as shown in Fig. 3 for the radial fin example.

Because the suppression of backscattered molecules from chamber walls is also important, consideration must be given to the fraction of efflux from a thruster that is able to return to the thruster vicinity after interacting with the cryopumping array. Such an analysis assuming only neutral components of the flow can prove helpful in designing array geometries to maximize pumping for a given application. For the smooth wall case, the fraction of molecules that returns to the thruster vicinity F_r is given by

$$F_{r,\mathrm{sw}} = (D_t/D_a)^2(1-\eta) \tag{13}$$

For the wedge fin array, the quantity in Eq. (13) is modified by[6]

$$F_{r,\mathrm{wf}} = F_{r,\mathrm{sw}}(D_{\mathrm{ts}}/D_a) \tag{14}$$

where D_{ts} is the diameter of the imaginary sphere in the center of the array to which the wedged fins are tangent. For example, in the MOLSINK facility, the value of D_{ts}/D_a was approximately 0.1, which gave an order of magnitude lower molecular backscatter fraction over a smooth-wall configuration. If a sticking coefficient of 0.7 is assumed on a 21-K pumping surface (Table 1), the MOLSINK F_r would be approximately 3.5×10^{-4} (Ref. 6).

The radial fin array fraction of backscattered molecules can be expressed by

$$F_{r,\mathrm{rf}} = (1-\eta)\{(w/2h)[w/(w+t)] + t/(w+t)\}(D_t/D_a)^2 \tag{15}$$

Note that Eq. (15) takes into consideration the finite thickness of the fins as scattering surfaces. Optimization of the pumping efficiency, that is, reduction of F_r, can be obtained by minimizing the geometric term in the brackets of Eq. (15). For a given thruster and facility size, the geometric term is optimized by an appropriate selection of the fin geometry. Figure 12 shows the geometric term as a function of the fin separation distance for a fin thickness of 0.32 cm and a fin length of 25.4 cm. Based on Eq. (15), the CHAFF-IV chamber F_r would be about 3.3×10^{-3} (Ref. 14). It is also evident from Fig. 12 that the cryofin geometry is not particularly critical (i.e., the separation distance can vary quite a bit without significant effects on the pumping efficiency), allowing for relaxed fabrication tolerances as long as a reasonable (±5 deg) radial profile is maintained.

Although the wedged fin array out performs cylindrical and radial fin configurations for neutral gas expansions, there are some issues associated with the design. First, wedged fin and cylindrical arrays are not acceptable for ion electric thruster operation because a large

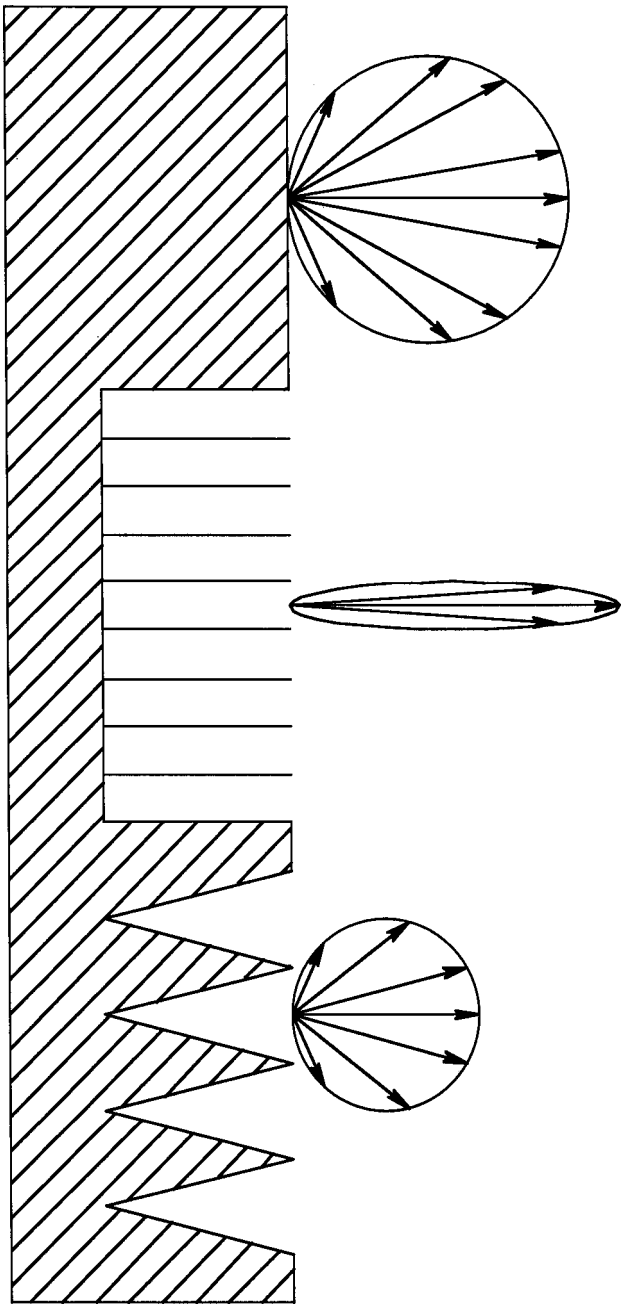

Fig. 11 Comparison of the distribution from a smooth wall (cylindrical), radial fin, and wedged fin cryopanel arrays.

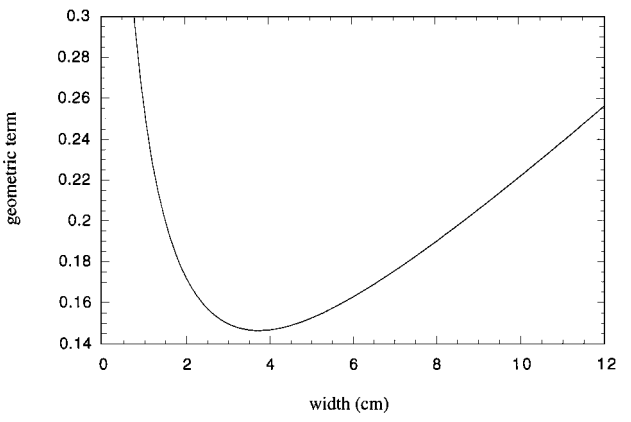

Fig. 12 Optimization of radial fin spacing for cryogenic arrays.

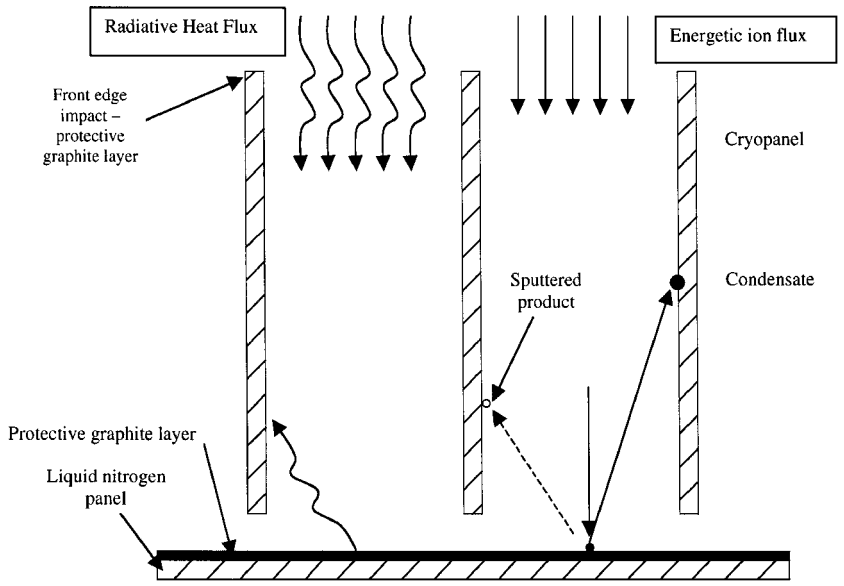

Fig. 13 Radial fin array geometry: a) Radiation interaction and b) ion bombardment.

fraction of the pumping surface area is exposed to energetic ion bombardment leading to sputtering of the pumping surfaces. Second, this configuration is exposed to the entire heat load of a thruster mounted in the facility. Energetic propellant molecules (even neutral species) impart all of their kinetic energy to the cryopumping surface, and infrared radiation emanating from an electric thruster will impinge directly on the array. The wedge fin and cylindrical geometrical configurations make it difficult to maintain adequate surface temperatures for efficient pumping.

Although the fraction of backscattered propellant molecules to the thruster is larger for a radial fin array then for a wedge fin array, the radial fin configuration offers some important benefits. First, the radial fin array can be manufactured with reasonable effort and cost relative to a wedge fin array.[14,15] Second, heat transfer from radiant heat and gas conduction can be minimized by allowing the radiation and propellant molecules to pass through the radial fin arrangement and impinge on a liquid nitrogen panel as shown in Fig. 13. The radiant energy is absorbed on the liquid nitrogen panel and the propellant molecules lose a significant fraction of their kinetic energy at the surface liquid nitrogen temperatures. The radial fin configuration also allows for more pumping surface area (roughly a factor of two) by opening pumping to both sides of the cryofins. Finally, the effects of sputtering for ion electric thruster operation can be minimized over the other cryopanel geometries, which will be discussed in the following section.

Of course, there are limitations to the amount of pumping surface area that a chamber can support. The most limiting factor is the capacity of the cryostat. Larger pumping areas imply more mass for the cryostat to cool. This can lead to very long cooldown times for the array. There are also limitations in terms of the pumping efficiency. As Fig. 12 shows, adding too many fins to increase the surface pumping area actually decreases the pumping efficiency.

Energetic Ion Sputtering

In a cryogenic pumping facility, there are two important sputtering populations to consider. The first is the sputtering of the array material itself. Figures 14 and 15 show the sputtering rates for various materials undergoing bombardment by energetic xenon ions. These results were obtained from the Monte-Carlo-based TRIM code.[31] The effects of the impact angle between the xenon ion and the surface can be seen in Figs. 14 and 15. These sputtered products can contribute to the background density and cause problems by coating critical components of a test article especially in the backflow regions.[32] As shown in Figs. 13 and 16, protecting surfaces with carbon or graphite films is beneficial. The problem associated with coating pumping surfaces with graphite films becomes one of heat transfer. The thermal conductivity of graphite and the existence

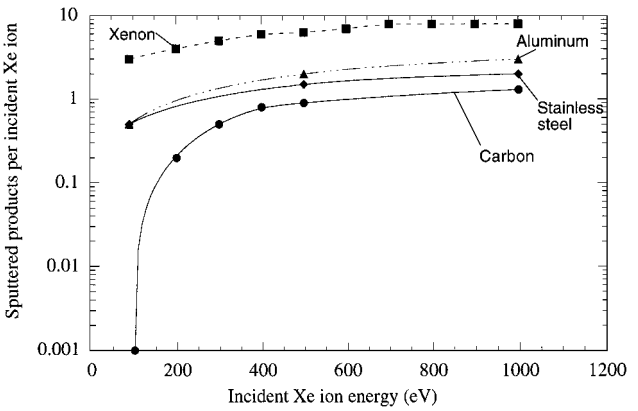

Fig. 14 Sputtering yield of various materials due to energetic xenon bombardment; TRIM code results for a glancing 5-deg impact angle.

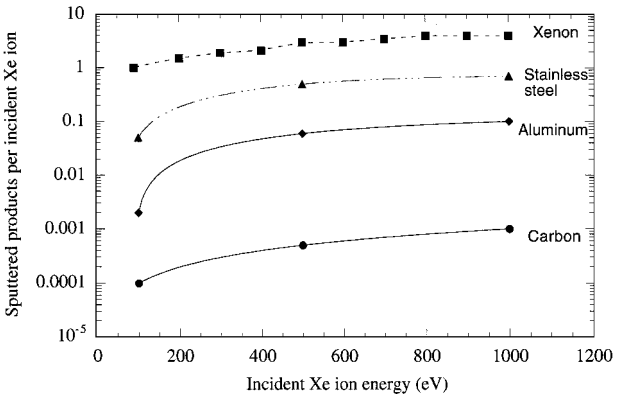

Fig. 15 Sputtering yield of various materials due to energetic xenon bombardment; TRIM code results for normal 90-deg impact angle.

of vacuum pockets between the graphite sheet and the cryopanel is such that the graphite can be at an elevated temperature with respect to the cryopanel and, thus, may not condense molecules effectively.

The second issue with energetic ion sputtering is the sputtering of solid xenon already condensed on the cryopanel. As Figs. 14 and 15 show, the sputtering yield for xenon ions impacting a xenon condensate is approximately 5 for ion energies of 300 eV, which will cause major issues with pumping efficiency unless handled properly. Again, the radial fin arrangement shown in Fig. 13 can be beneficial.

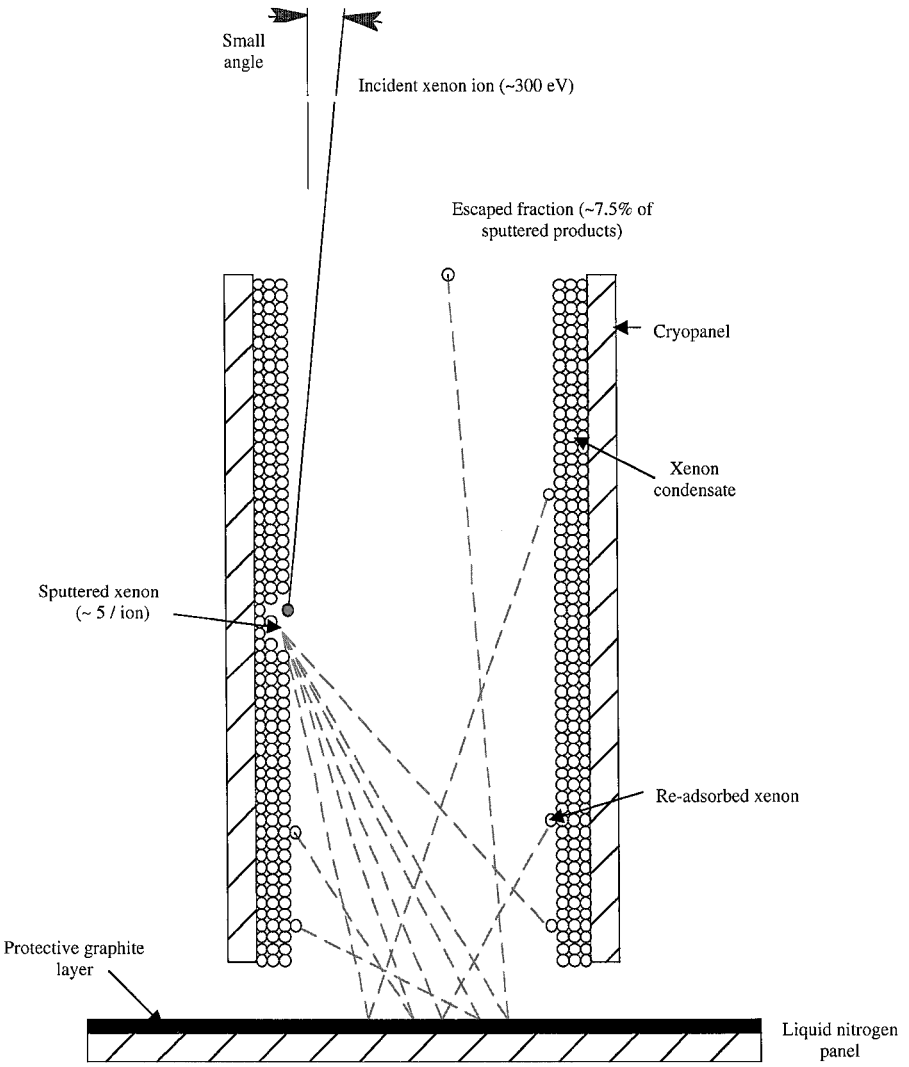

Fig. 16 Desorption of cryogenic condensate due to energetic ion bombardment in an open radial fin arrangement.

Because xenon will not condense on the graphite protective surfaces, the flow through pattern of the ions with respect to the pumping array should not cause sputtered xenon condensate. There will, however, be some side ion impacts to the pumping panels. In the radial fin geometry, the motion of the sputtered condensate is expected to be toward the liquid nitrogen panel due to momentum transfer from the highly directional ions. The sputtered condensate molecules then experience a similar line-of-sight reduction due to the radial fin geometry as shown in Fig. 16.

The benefits of the radial fin arrangement are shown in Fig. 13. In this configuration, the propellant ions are allowed to pass through the fins and interact with a graphite sheet placed before the liquid nitrogen panel. The liquid nitrogen panel is required to reduce the heat transfer from the outer chamber wall to the cryopanel array. Sputtered products formed at the graphite layer then have a limited line of sight back to the thruster due to the radial fin arrangement; however, there may still be an issue with sputtering from the finite thickness of the radial fin. Because pumping is not desired along the fin thickness due to xenon condensate sputtering, these edges can also be coated with a graphite layer to minimize sputtering of the radial fin material.

Incondensable Pumping

Some level of pumping is necessary to remove incondensable gases such as hydrogen and helium that the cryogenic array can not capture. Hydrogen and helium are present in the facility from the ambient laboratory atmosphere, but they can also be introduced as propellant species in arcjets or resistojets, as combustion products in chemical thrusters, and as impurities in propellant supply bottles. The incondensable molecules can be removed by a variety of commercial pumps of varying complexity and cost. The size of the incondensable pump depends on the circumstances of the experiment. For example, a large molecular hydrogen background might be expected from the operation of a hydrazine thruster or an ammonia arcjet, and very little hydrogen or helium would be expected for a typical xenon ion thruster fed by an ultra-high-purity bottle.

It is best to select an oilless pump that minimizes the possibility of contaminating the facility. For example, magnetic bearing turbomolecular pumps are ideal for this situation, although they can be expensive if high pumping rates are required. Cryosorption pumps that utilize zeolites to pump hydrogen and helium are also very effective, but they are susceptible to oil and water vapor contamination. For extremely high flow rate applications, large oil diffusion pumps may be considered. When considering these pumps, the oil backstreaming rate must be a factor. Although these pumps operate by vaporizing silicon-based oils, effective oil traps minimize the backstreaming rate into the facility, but these traps also severely limit the pumping capacity.

Summary

The most critical design parameters for ground-based spacecraft–thruster interaction facilities is the facility's pumping speed and the mitigation of propellant backscattering from chamber surfaces. Large pumping rates are required to minimize background gas number densities. Currently, cryopumping offers the only means to obtain adequate pumping rates for interaction studies. In cryopumping

schemes, the pumping rate is proportional to the amount of surface area that is cooled to cryogenic temperatures. The concept of TCP maximizes the amount of pumping area available. The cryopumping array design is also critical to the pumping efficiency or minimization of surface backscattering. For facilities that do not intend to operate ion electric thrusters, a wedge fin design maximizes efficiency. Facilities that plan on operating ion thrusters should use a radial fin design to minimize the impact of sputtered products and heat transfer from the thruster.

Some general facility design guidelines are outlined. First, maximize cryogenic array pumping area as much as possible. The amount of array area is restricted by cost, cryostat load capability, maximum pump-down time, and chamber size. The array size can be maximized by the utilization of a fin design (wedge or radial). Second, minimize the geometric term given in Eq. (15) for a radial fin array. In general, higher panels (increased h) and smaller panel thickness t aid in maximizing pumping efficiency. The panel dimensions are limited by their heat transfer capabilities, manufacturing limitations, and cost. Third, provide some level of pumping for incondensable gases. Cryosorption material (zeolites) are the lowest contamination risk approach but have saturation limitations. Alternative approaches exist. If large flow rates of incondensable gases are expected, the most cost-effective means of efficient pumping is diffusion pumps. These pumps should be cold trapped to minimize oil backstreaming into the chamber. Finally, the cost of designing and building a space simulation facility is not trivial; therefore, the facility should be as flexible as possible in terms of the types of experiments that can be performed. To this end, the designer should always opt for the highest possible pumping rate that can be absorbed by the available budget.

Acknowledgments

This work was partially funded by the Air Force Office of Scientific Research and the Air Force Research Laboratory's Propulsion Directorate. The author would like to acknowledge E.P. Muntz and Fred Lutfy for their important contributions to this work. The figure making talents of Jeffery Brown are also appreciated.

References

[1]Randolph, T., Pencil, E., and Manzella, D., "Far-Field Plume Contamination and Sputtering of the Stationary Plasma Thruster," AIAA Paper 94-2855, June 1994.

[2]Lumpkin, F., Le Beau, G., and Stuart, P., "A CFC/DSMC Analysis of Plumes and Plume Impingement During Shuttle/Mir Docking," AIAA Paper 95-2034, June 1995.

[3]Roy, R., Hastings, D., and Gatsonis, N., "Numerical Study of Spacecraft Contamination and Interactions by Ion-Thruster Effluents," *Journal of Spacecraft and Rockets*, Vol. 33, No. 4, 1996, pp. 535–542.

[4]Boyd, I., Beattie, D., and Cappelli, M., "Chamber Effects on Plume Expansion for a Low-Power Hydrogen Arcjet," International Electric Propulsion Conf., Rept. IEPC-93-126, Sept. 1993.

[5]Manzella, D., Penko, P., Witt, K., and Keith, T., "Test-Cell Pressure Effects on the Performance of Resistojets," *Journal of Propulsion and Power*, Vol. 7, No. 2, 1991, pp. 269–274.

[6]Stephens, J. B., "Space Molecular Sink Simulator Facility Design," Jet Propulsion Lab., NASA TR 32-901, California Inst. of Technology, Pasadena, CA, March 1966.

[7]Simon, W., "Nozzle Exhaust Plume Backscatter Experiment Using the JPL Molsink Facility," *Jet Propulsion Laboratory Quarterly Technical Review*, Vol. 1, No. 4, 1972, pp. 89–96.

[8]Simon, W., "Plume Backscatter Measurements Using Quartz Crystal Microbalances in JPL Molsink," Jet Propulsion Lab., NASA TM 33-540, California Inst. of Technology, Pasadena, CA, May 1972.

[9]Chirivella, J. E., "Operation of Small Rocket Engines in the JPL High-Vacuum Molecular Space Simulator (Molsink)," *Jet Propulsion Laboratory Quarterly Technical Review*, Vol. 3, No. 1, 1973, pp. 1–13.

[10]Hufenbach, B., Dettleff, G., Bottcher, R., Trinks, H., Cheoux-Damas, P., Theroude, C., and Castegon, S., "European Activities in Plume Testing," AIAA Paper 97-3301, July 1997.

[11]Welch, K., *Capture Pumping Technology*, 1st ed., Pergamon, New York, 1991, p. 308.

[12]Dettleff, G., and Plahn, K., "Initial Experimental Results form the New DLR- High Vacuum Plume Test Facility STG," AIAA Paper 97-3297, July 1997.

[13]Ketsdever, A., Young, M., Jamison, A., Eccles, B., and Muntz, E. P., "Investigation of the Unique Cryogenic Pumping System of the CHAFF-IV Spacecraft-Thruster Interaction Facility," 22nd International Rarefied Gas Dynamics Symposium, Paper 10013, July 2000.

[14]Lutfy, F. M., Vargo, S. E., Muntz, E. P., and Ketsdever, A. D., "The David P. Weaver Collaborative High Altitude Flow Facility's CHAFF-4 for Studies of Spacecraft Propulsion Plumes and Contamination," AIAA Paper 98-3654, July 1998.

[15]Lutfy, F. M., Green, A. A., Muntz, E. P., and Ketsdever, A. D., "Investigation of the Operational Envelope of the CHAFF-IV Plume and Contamination Thermospheric Flow Simulator," AIAA Paper 99-2719, June 1999.

[16]Muntz, E. P., Hamel, B. B., and Maguire, B. L., "Some Characteristics of Exhaust Plume Rarefaction," *AIAA Journal*, Vol. 8, No. 9, 1970, pp. 1651–1658.

[17]Ketsdever, A. D., "The Production of Energetic Atomic Beams Via Charge Exchange for the Simulation of the Low-Earth Orbit Environment," Ph.D. Dissertation, Dept. of Aerospace Engineering, Univ. of Southern California, Los Angeles, CA, Aug. 1995.

[18]Dettleff, G., "Plume Flow and Plume Impingement in Space Technology," *Progress in Aerospace Science*, Vol. 28, No. 1, 1991, pp. 1–71.

[19]Dettleff, G., and Plahn, K., "Experimental Investigation of Fully Expanding Free Jets and Plumes," *Rarefied Gas Dynamics*, Vol. 2, edited by R. Brun, R. Campargue, R. Gatignol, and J.-C. Lengrand, Cépadués Éditions, Toulouse, France, 1999, pp. 607–614.

[20]Randolph, T., Day, M., Kim, V., Kaufman, H., Zhurin, V., and Kozubsky, K., "Facility Effects on SPT Thruster Testing," International Electric Propulsion Conf., Rept. IEPC-93-093, Sept. 1993.

[21]Zhurin, V., Kahn, J., Kaufman, H., Kozubsky, K., and Day, M., "Dynamic Characteristics of Closed Drift Thrusters," International Electric Propulsion Conf., Rept. IEPC-93-095, Sept. 1993.

[22]Hasted, J. B., *Physics of Atomic Collisions*, 2nd ed., Butterworths, London, 1972, p. 10.

[23]Pullins, S., Chiu, Y., Levandier, D., and Dressler, R., "Ion Dynamics in Hall Effect and Ion Thrusters: $Xe^+ + Xe$ Symmetric Charge Transfer," AIAA Paper 2000-0603, Jan. 2000.

[24]Samanta Roy, R., and Hastings, D., "Modeling of Ion Thruster Plume Contamination," AIAA Paper 93-2531, June 1993.

[25]Suzuki, M., Taniguchi, T., Yoshimura, N., and Tagashira, H., "Momentum Transfer Cross Sections of Xenon Deduced from Electron Drift Velocity Data," *Journal of Physics D: Applied Physics*, Vol. 25, No. 1, 1992, pp. 50–56.

[26]McLean, C. H., and Lesky, O., "Development of a Helium Cryopumped Facility to Evaluate Hall Effect Thrusters," International Electric Propulsion Conf., Rept. IEPC-97-135, Aug. 1997.

[27]Lasgorceix, P., Raffin, M., Perot, C., Lengrand, J. C., Dudeck, M., Beltan, T., and Cadiou, A., "PIVOINE: A Facility for the Investigation of Rarefied Xenon Plasma Jet," *Rarefied Gas Dynamics*, edited by C. Chen, Peking Univ. Press, Beijing, 1997, pp. 952–956.

[28]Dushman, S., and Lafferty, J., *Scientific Foundations of Vacuum Technique*, 2nd ed., Wiley, New York, 1962, pp. 111–116.

[29]Santeler, D., Holkeboer, D., Jones, D., and Pagano, F., "Vacuum Technology and Space Simulation," SP-105, NASA, March 1966, p. 153.

[30]Garner, C., Polk, J., Brophy, J., and Goodfellow, K., "Methods for Cryopumping Xenon," AIAA Paper 96-3206, July 1996.

[31]Ziegler, J., Bierback, J., and Littmark, U., *The Stopping Range of Ions in Solids*, Vol. 1, 1st ed., Pergamon, New York, 1985, pp. 202–226.

[32]Pencil, E., "Preliminary Far-Field Plume Sputtering Characterization of the Stationary Plasma Thruster (SPT-100)," International Electric Propulsion Conf., Rept. IEPC-93-098, Sept. 1993.

I. D. Boyd
Associate Editor